Immunity
Article

Distinct and Nonredundant In Vivo Functions of IFNAR on Myeloid Cells Limit Autoimmunity in the Central Nervous System

Marco Prinz,[1,2,9,*] Hauke Schmidt,[2,9] Alexander Mildner,[1,2] Klaus-Peter Knobeloch,[1,3] Uwe-Karsten Hanisch,[2] Jenni Raasch,[2] Doron Merkler,[2] Claudia Detje,[4] Ilona Gutcher,[5] Jörg Mages,[6] Roland Lang,[6] Roland Martin,[7] Ralf Gold,[8,10] Burkhard Becher,[5] Wolfgang Brück,[2,8] and Ulrich Kalinke[4,*]
[1]Department of Neuropathology, University of Freiburg, D-79106 Freiburg, Germany
[2]Institute of Neuropathology, Georg August University, D-37099 Göttingen, Germany
[3]Institute of Molecular Pharmacology, Department of Molecular Genetics, D-12207 Berlin, Germany
[4]Division of Immunology, Paul-Ehrlich-Institut, D-63225 Langen, Germany
[5]Department Neurology/Neuroimmunology Unit, Universitätsspital, CH-8091 Zurich, Switzerland
[6]Institute of Medical Microbiology, Immunology and Hygiene, Technische Universität München, D-81675 Munich, Germany
[7]Institute of Neuroimmunology and for Clinical Multiple Sclerosis Research, University, D-20251 Hamburg, Germany
[8]Institute for Multiple Sclerosis Research, Georg August University, D-37099 Göttingen, Germany
[9]These authors contributed equally to this work.
[10]Present address: Department of Neurology, St. Josef Hospital, Ruhr University Bochum, D-44791 Bochum, Germany.
*Correspondence: marco.prinz@uniklinik-freiburg.de (M.P.), kalul@pei.de (U.K.)
DOI 10.1016/j.immuni.2008.03.011

SUMMARY

The action of type I interferons in the central nervous system (CNS) during autoimmunity is largely unknown. Here, we demonstrate elevated interferon beta concentrations in the CNS, but not blood, of mice with experimental autoimmune encephalomyelitis (EAE), a model for CNS autoimmunity. Furthermore, mice devoid of the broadly expressed type I IFN receptor (IFNAR) developed exacerbated clinical disease accompanied by a markedly higher inflammation, demyelination, and lethality without shifting the T helper 17 (Th17) or Th1 cell immune response. Whereas adoptive transfer of encephalitogenic T cells led to enhanced disease in *Ifnar1*$^{-/-}$ mice, newly created conditional mice with B or T lymphocyte-specific IFNAR ablation showed normal EAE. The engagement of IFNAR on neuroectodermal CNS cells had no protective effect. In contrast, absence of IFNAR on myeloid cells led to severe disease with an enhanced effector phase and increased lethality, indicating a distinct protective function of type I IFNs during autoimmune inflammation of the CNS.

INTRODUCTION

Multiple sclerosis (MS) is considered to be an inflammatory demyelinating disease of the central nervous system (CNS), and its etiology remains unclear (Steinman, 1996). This condition is represented in the well-established animal model for brain inflammation and MS, known as experimental autoimmune encephalomyelitis (EAE), which is a vital tool to study the neuroimmunological events related to the disease (Owens et al., 2001) and resembles many facets of MS (Gold et al., 2006).

Therapeutic application of interferon gamma (IFN-γ) induced acute relapses in MS patients (Panitch et al., 1987), supporting the notion that proinflammatory T helper type 1 (Th1) cell cytokines play a crucial role in the immunopathogenesis of MS. In contrast, the type I interferon beta (IFN-β) reduces the frequency of clinical exacerbations by about 35% and delays the progression of disability in relapsing-remitting MS. Similarly, the lack of the IFN-β gene in mice strongly enhanced the course of EAE (Teige et al., 2003), and type I interferons can downregulate EAE in mice and rats (Brod and Khan, 1996; Brod and Burns, 1994), indicating that IFN-β modulates the disease activity in MS and EAE in a similar fashion.

Regarding the underlying mechanism, earlier studies have suggested several possibilities, including inhibition of Th1 cell development (McRae et al., 1998), induction of Th2 cell immune deviation (Kozovska et al., 1999), restoration of function of the disrupted blood-brain barrier (Stone et al., 1995), and downregulation of IFN-γ-induced expression of class II major histocompatibility complex (MHC) molecules on CNS cells (Satoh et al., 1995). In the light of recent data on IFN-β-induced gene profiles (Satoh et al., 2006; Wandinger et al., 2001), however, it is generally accepted that IFN-β reveals extremely complex actions that cannot only be reduced to a simple Th2 cell shift (Frohman et al., 2006).

To date, therapeutic intervention using IFN-β is a major treatment option for MS. However, in up to one-third of the cases, the efficiacy of IFN-β therapy ceases after one year, partly because of the fact that many of these patients develop autoantibodies against IFN-β (Waubant et al., 2003). Furthermore, a substantial proportion of the patients discontinue IFN-β treatment because of multiple serious side effects, such as skin reactions, flu-like symptoms, leukocytopenia, liver dysfunction, depression, elevated suicide rate, and amenorrhea (Neilley et al., 1996).

These adverse effects stress the need to better understand how IFN-β actually functions on the molecular and cellular level in an in vivo setting. Previous studies relied on simplified in vitro

experiments. Progress with the EAE model, on the other hand, was hampered by the fact that the respective receptor of type 1 interferons (IFN-αs and IFN-β), IFNAR, is broadly expressed by virtually all cell types and tissues, including immune cells (Pogue et al., 2004), endothelial cells (Floris et al., 2002), and CNS-resident neurons and glia (Okada et al., 2005; Heine et al., 2006).

To identify the actual cell type targeted by disease-associated IFN-β locally produced in the brain, we conditionally deleted IFNAR from the CNS, lymphocytes, or myeloid cells and studied the pathogenesis of CNS autoimmunity in such mice. Our investigations provide insights into disease-limiting mechanisms that might open new avenues to more cell-specific IFN-β-based therapies minimizing severe adverse effects. Despite being broadly expressed, INFAR was determined to have a unique role on myeloid cells for modulating CNS autoimmunity.

RESULTS

Local IFN-β Production and IFNAR Signaling within the CNS during Autoimmunity

We first assessed endogenous IFN-β production in the CNS and blood of $MOG_{35–55}$ immunized mice by an enzyme-linked immunoabsorbent assay (ELISA) method on day 7, when animals were still free of disease symptoms (score 0), and on day 18, when animals presented with full EAE symptoms (scores > 1.5). Sick individuals showed increased amounts of IFN-β levels in the CNS, whereas IFN-β in the blood of both groups was below the detection limit (Figure 1A).

To assess IFNAR signaling triggered by endogenously produced IFN-β, we extracted total RNA from the spinal cord of healthy (score 0), moderately sick (scores 0.5–1.5), and severely affected (scores > 2.5) mice and monitored the expression of IFNAR-dependent genes by RNA blotting. Even in moderately sick mice, enhanced hybridization signals were found for interferon regulatory factor 1 (IRF1), interferon regulatory factor 7 (IRF7), interferon stimulated gene 15 (ISG 15), and 2′,5′oligoadenylatsynthetase (2′,5′OAS) (Figure 1B). Collectively, these data indicate that even at the onset of the first clinical symptoms, when leukocyte influx can first be monitored, IFN-β is produced locally in the brain in biologically relevant quantities.

Disease-Modulating Role of IFNAR during the Effector Phase of EAE

To examine the impact of IFNAR signaling on the disease course of EAE, we immunized *Ifnar1*$^{-/-}$ and wild-type (WT) mice. All animals developed EAE with an incidence of 100% and a similar mean disease onset (Table S1 available online). However, in *Ifnar1*$^{-/-}$ animals, the effector phase of disease was changed dramatically, with an increased lethality rate and an augmented mean maximal clinical score (Figure 2A, Table S1, Movies S1 and S2).

IFNAR-deficient spinal cords showed histologically at 35 days after immunization a plethora of infiltrating MAC-3^{+} macrophages and microglia in the submeningeal and perivascular space, as well as in the CNS parenchyma, which were, upon quantification of the histological sections, significantly upregulated ($p < 0.05$) (Figures 2B and 2C right panel). Importantly, this increased influx of macrophages was accompanied by an

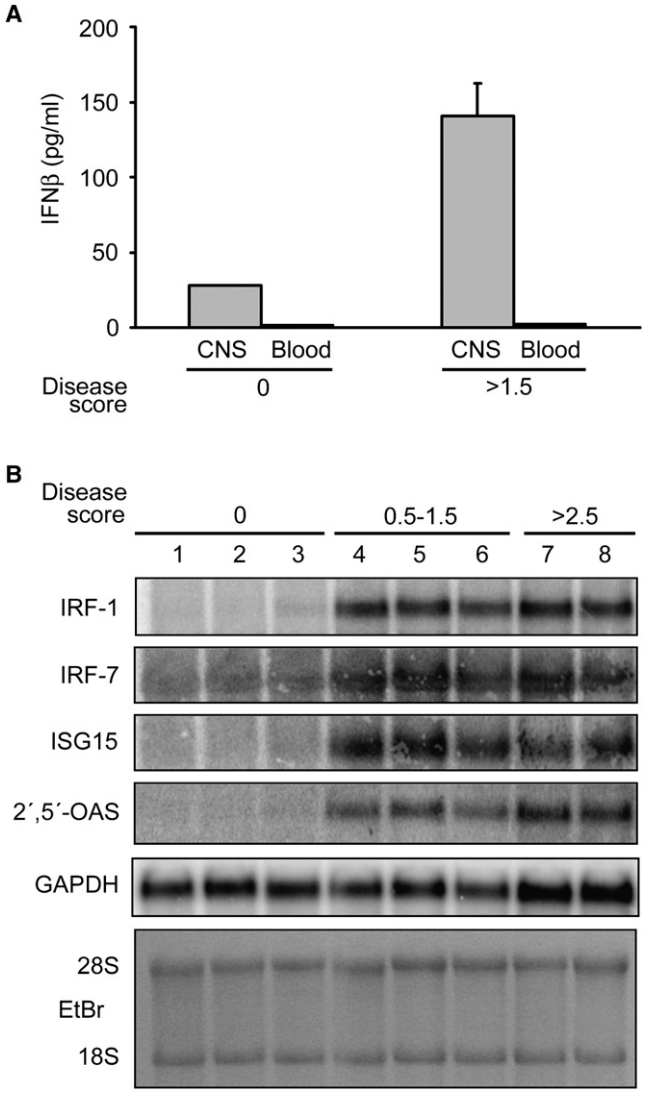

Figure 1. CNS-Endogenous Induction of IFN-β and IFNAR Signaling during Autoimmune Disease

(A) Measurement of IFN-β production in the CNS (gray bars) and blood samples (black bars) of immunized, nonsick animals (score 0) or sick animals (score > 1.5). Data represent the means out of four animals in each group ± the standard error of the mean (SEM).

(B) RNA blot analysis showing disease-associated induction of IFNAR-dependent genes in the CNS of eight individual mice that are either healthy (immunized, score 0), slightly (score 0.5–1.5) or severely EAE sick (score > 2.5). IFNAR-induced genes were interferon regulatory factor 1 (IRF1), interferon regulatory factor 7 (IRF7), 2′-5′ oligoadenylatsynthetase (2′,5′ -OAS), and interferon-stimulated gene 15 (ISG15).

invasion of numerically unchanged CD3^{+} lymphocytes. The myelin damage, however, was increased in *Ifnar1*$^{-/-}$ animals (Figure 2C, left panel, $p < 0.05$). This distinct pathological infiltration reflected clinical characteristics of *Ifnar1*$^{-/-}$ mice showing increased disease burden.

Th17 cells are now widely believed to be the main pathogenic population during autoimmune CNS inflammation (Steinman, 2007). We therefore quantified interleukin-17 (IL-17)-producing myelin oligodendrocyte glycoprotein (MOG)-reactive T cells in

the CNS at day 14 as well as in lymph node cells at days 7 and 14 (Figure 2D, Figure S1). Enzyme-linked immunospot analysis did not show any apparent changes in the IL-17, IL-4, and IFN-γ profiles in antigen-specific T cells. For further determination of the impact of IFNAR expression on the cytokine profile within the CNS, mice were sacrificed at the disease peak, and expression of chemoattractant factors and cytokines were examined by real-time polymerase chain reaction (PCR) (Figure 2E). Despite a trend toward generally elevated amounts of cytokines in IFNAR-deficient mice, IFN-γ, IL-12p35, STAT6, IL-13, TGF-β1, IL-6, and IL-23p19 were not significantly increased, suggesting that more severe EAE in the absence of IFNAR is not linked to a certain Th1, Th2, or Th17 cell bias throughout the disease course. In contrast, chemokines recruiting monocytes and macrophages such as CCL2 and CXCL10 were found to be increased in *Ifnar1*$^{-/-}$ mice ($p < 0.05$). These data revealed that IFNAR is important for the modulation of the effector phase of autoimmunity, and its absence facilitates macrophage invasion into the CNS accompanied by higher demyelination and production of chemokines without shifting the T cell profile.

CNS-Specific IFNAR Expression Is Dispensable for the Induction and Progression of EAE

To assess the role and function of IFNAR during the EAE effector phase, which essentially occurs within the CNS, encephalitogenic MOG-reactive lymphocytes were isolated from WT mice and adoptively transferred into either WT or *Ifnar1*$^{-/-}$ recipient mice. *Ifnar1*$^{-/-}$ mice developed EAE with earlier disease onset and increased severity, as well as higher incidence rate ($p < 0.05$, Figure 3 and Table S2). These data indicate that IFNAR is involved in the local maintenance of encephalitogenicity during the effector phase of EAE within the CNS.

To determine whether IFNAR engagement of CNS-resident cells limits the progression of autoimmune inflammation, we crossed conditional (floxed) IFNAR mice with a transgenic mouse line expressing the Cre recombinase under the control of the nestin promoter. Southern-blot analysis of DNA isolated from different tissues of an *Ifnar1*$^{fl/fl}$ NesCre mouse showed efficient deletion of the gene fragment flanked by loxP in the CNS tissue and isolated astrocytes, whereas recombination was absent in the spleen and in primary microglia (Figure 4A).

Upon immunization, all *Ifnar1*$^{fl/fl}$ NesCre mice developed neurological signs of disease such as tail weakness and paralysis, starting about 13–16 days after immunization. (Figure 4B, Table S3), indicating that the priming phase of disease was unaltered. Furthermore, the mean maximal scores were similar in both groups, suggesting that IFNAR expression on CNS cells is dispensable in EAE. Examination of the CNS revealed no obvious differences in either the pattern of mononuclear infiltration or the amount of macrophages or microglia, and T lymphocytes (Figure 4C). Because the Cre transgene is active in all neuroectodermal cells, we also examined disease-associated pathology in axons (Figure 4D), oligodendrocytes (Figure 4E), and astrocytes (Figure 4F) and found no marked changes (Figures 4D–4F). Overall, these data indicated that the brain-specific IFNAR is not an essential modulator of the degree and composition of inflammation, demyelination, and axonal damage during sterile autoimmune CNS disease.

IFNAR Engagement on Lymphocytes Has No Impact on T Cell Priming or EAE Development

We further studied the direct impact of IFN-β on lymphocytes in mice with a T cell-specific IFNAR deletion (*Ifnar1*$^{fl/fl}$ CD4Cre) and their respective negative littermate controls (*Ifnar1*$^{fl/fl}$). The analyzed groups developed disease with a similar incidence and a comparable mean disease onset and severity (Figure 5, Table S3). Notably, there were 3 days during the priming phase in which T cell-specific *Ifnar1*$^{-/-}$ mice had a higher clinical score ($p < 0.05$, Figure 5B). Spinal cord sections, however, revealed a comparable amount of macrophages and microglia and T lymphocytes in *Ifnar1*$^{fl/fl}$ CD4Cre mice (Figure 5C). Accordingly, myelin damage was similar in this line.

To determine whether loss of IFNAR on T cells had an overall impact on antigen (Ag)-driven responses, we immunized mice with either $MOG_{35–55}$ peptide or keyhole limpet haemocyanine (KLH) emulsified in complete freund adjuvant (CFA) and assessed the capacity of lymphocytes to respond to their cognate Ag in a recall assay. Lymphocytes from *Ifnar1*$^{fl/fl}$ CD4Cre mice developed comparable proliferative responses and produced similar amounts of encephalitogenic IL-17 (Figures 5D and 5E). In addition, in *Ifnar1*$^{fl/fl}$ CD4Cre mice, CNS-infiltrating T lymphocytes revealed unchanged amounts of the activation markers CD62L and CD44 (Figure 5F). These results clearly demonstrated that IFNAR triggering of T cells had no impact on the induction and progression of CNS autoimmunity.

Because B cells also carry the IFNAR (Pogue et al., 2004), B cell-specific *Ifnar1*$^{-/-}$ mice (*Ifnar1*$^{fl/fl}$ CD19Cre) and their respective littermate controls (*Ifnar1*$^{fl/fl}$) were challenged with MOG in CFA. No clinical differences were observed between the groups regarding their clinical parameters Figure S3, Table S3). As expected, concomitant CNS pathology was similar in terms of distribution as well as amount of infiltrating macrophages, T lymphocytes, and demyelination (Figure S3C).

To test whether B cells could produce antigen-specific IL-10 in the absence of IFNAR, we purified splenic B cells from mice that were in the effector phase of EAE. To ensure B cell-receptor crosslinking, we coated tissue-culture wells with $MOG_{35–55}$ before adding the purified B cells. B cells incubated with the antigen alone did not produce IL-10. Addition of an agonistic CD40 antibody to the cultures, however, resulted in production of IL-10, which could be further increased in combination with the MOG antigen (Figure S3D). Notably, this B cell-specific IL-10 production was independent of the presence of IFNAR. Taken together, these results clearly show that IFNAR engagement on lymphocytes by endogenous type I IFN had no impact on EAE development.

Distinct and Nonredundant In Vivo Functions of IFNAR on Myeloid Cells Determine Disease Course

Myeloid cells are potential targets for endogenously produced IFN-β and might therefore function as cells limiting disease during CNS autoimmunity. To address this question experimentally, we first analyzed *Ifnar1*$^{fl/fl}$ LysMCre mice for cell specificity of IFNAR deletion (Figure 6A, Figures S2A and S4). As expected, $CD11b^+$ cells showed a strong deletion of IFNAR on both the DNA and protein level. Because the LysM Cre transgene is potentially expressed in many myeloid cell types, we characterized IFNAR depletion in specific $CD11b^+$ subsets (Figure S2B). We

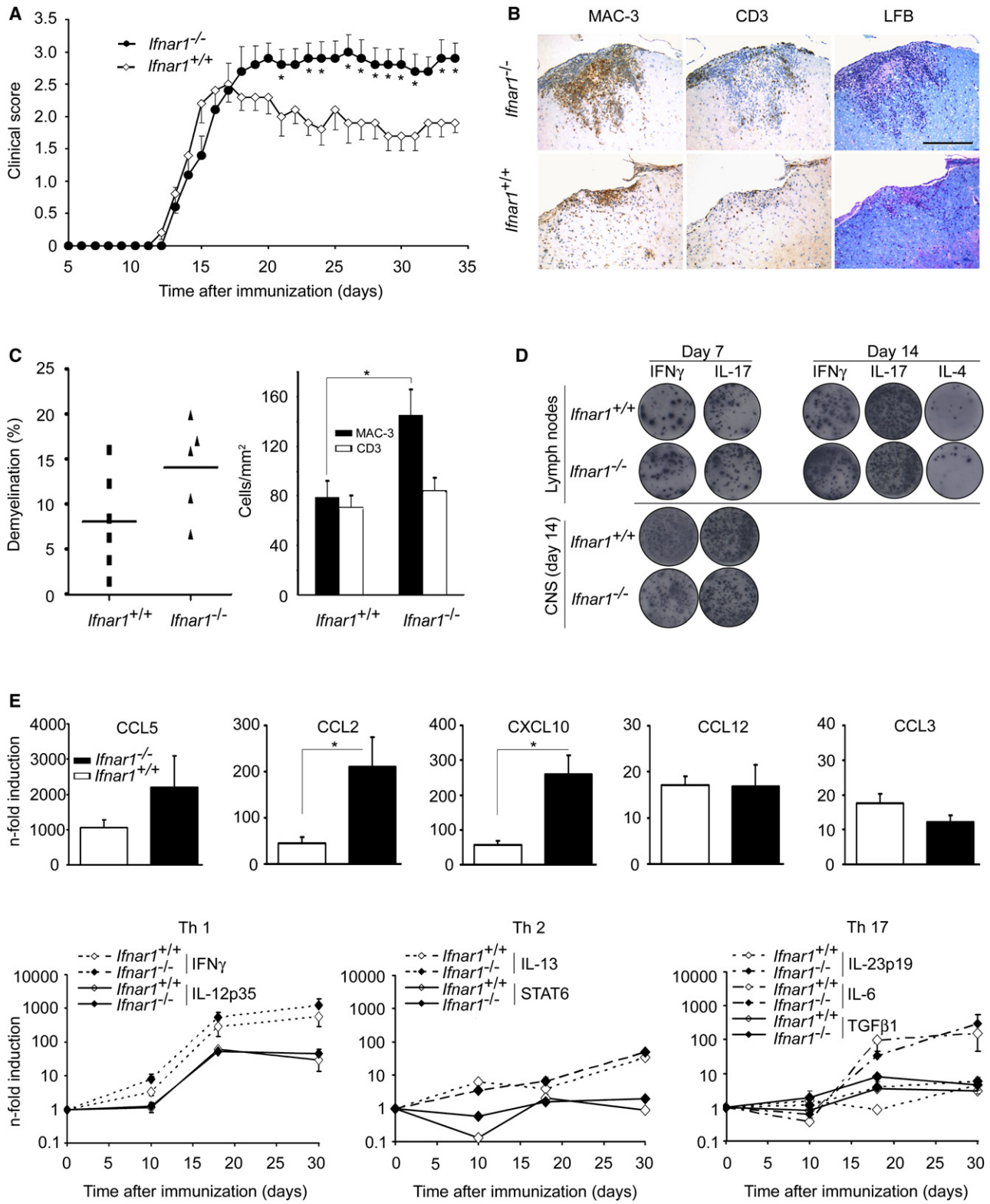

Figure 2. IFNAR Signaling Is Critical for the Effector Phase of Disease, CNS Pathology, and the Induction of Myeloattractants

(A) EAE was induced by active immunization of *Ifnar1*$^{+/+}$ (open squares) and *Ifnar1*$^{-/-}$ (filled circles) mice, and disease was scored as described in the Experimental Procedures. Each data point represents the mean of at least seven animals. Statistically significant data points are marked with asterisks ($p < 0.05$). (B and C) Characterization of infiltrates and demyelination in IFNAR-deficient mice. (B) shows histology of spinal cord sections with CD3 for T lymphocytes, MAC-3 for macrophages, and luxol fast blue (LFB) for demyelination (scale bar represents 200 μm). (C) shows quantification of demyelination

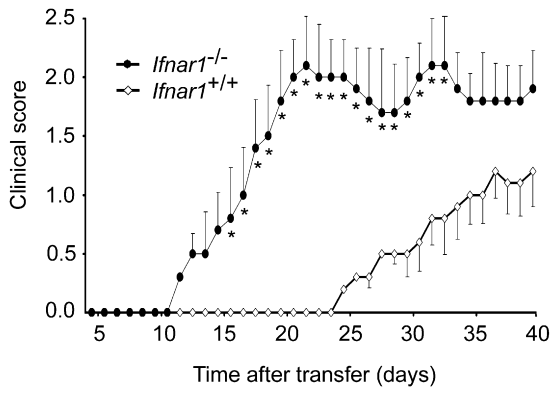

Figure 3. Encephalitogenic T Cells Are More Effective at Inducing EAE When Transferred into IFNAR-Deficient Hosts

Clinical score over time after adoptive transfer of MOG-reactive T cells into *Ifnar1*$^{-/-}$ (filled circles) or *Ifnar1*$^{+/+}$ (open squares). Data shown are from one representative experiment of three individual experiments with at least five mice per group. Asterisks indicate statistical significance ($p < 0.05$).

found substantial IFNAR deletion on CD11b^{+}Ly-6C^{lo} resident monocytes (r monocytes) as well as on CD11b^{+}Ly-6C^{hi} inflammatory blood monocytes (i monocytes) but importantly not on CD11c^{+}CD11b^{-}B220^{+} plasmacytoid dendritic cells (pDCs) or CD11c^{+}CD11b^{+}B220^{-} myeloid DCs (mDCs). CD11b^{+}Gr-1^{+} granulocytes, however, revealed an IFNAR deletion as well. Notably, deletion of IFNAR led to a strong decrease of phosphorylated STAT1 protein in CD11b^{+} splenocytes upon stimulation with IFN-β in *Ifnar1*$^{fl/fl}$ LysMCre cells compared to WT CD11b^{+} cells (Figure S2C).

After immunization of mice, a similar disease onset with a disease incidence comparable to WT mice was observed (Figure 6B, Table S3). Surprisingly, clinical disease was clearly aggravated during the effector phase in *Ifnar1*$^{fl/fl}$ LysMCre mice, leading to a lethality rate of 33%, whereas all *Ifnar1*$^{fl/fl}$ mice survived ($p < 0.05$). Accordingly, the mean clinical score was significantly higher in *Ifnar1*$^{fl/fl}$ LysMCre animals ($p < 0.05$, Figure 6B, Table S3). The phenotype of this line largely mirrors the disease course seen in *Ifnar1*$^{-/-}$ mice. Importantly, the generation of encephalitogenic MOG-specific T lymphocytes was unaltered even at early time points in *Ifnar1*$^{fl/fl}$ LysMCre mice, indicating that LysM expressing IFNAR^{+} cells were not essential for priming (Figure 6C, Figure S5).

We next used quantitative real-time PCR analysis to determine the expression of proinflammatory mediators in the CNS of myeloid cell-specific *Ifnar1*$^{-/-}$ mice at the peak of disease (Figure S6). Among factors tested, CCL2 and TNFα were upregulated in the CNS of IFNARfl/fl LysMCre animals. We further measured surface marker expression on CNS infiltrating CD11b^{+} cells. We found more MHC class II-expressing CD11b^{+} cells in the CNS showing either Ly-6C^{hi} or Ly-6C^{lo} expression and CD45^{hi} or CD45^{lo}, indicating the involvement of several myeloid MHC class II^{+} cell types (Figure 6D).

In order to clarify whether engagement of IFNAR on macrophages and microglia modulates CNS pathology, we measured the amount of degraded myelin protein (dMBP) in MAC-3^{+} macrophages and microglia and found significantly increased numbers of deposits in the absence of IFNAR (Figure 6E). To test further whether IFNs can change the uptake of myelin by macrophages, we challenged isolated macrophages with IFN-β in vitro (Figure 6F). We found that exogenously added IFN-β was able to modulate myelin uptake by macrophages. Myelin uptake was significantly reduced after incubation with IFN-β, indicating that IFNAR-mediated signaling is a regulator of myelin phagocytosis on cellular level. Further, exogenously added IFN-β revealed impaired MHC class II downregulation in IFN-γ-stimulated *Ifnar1*$^{-/-}$ macrophages that was largely dependent on the presence of Tyk2, a member of the Jak family kinases known to be crucial for the receptor signal transduction by IFNs (Figure 6G).

To determine how the lack of IFNAR on myeloid cells shapes the immune profile of macrophages, we tested the chemokine pattern in response to the IFN-β inducer LPS alone and in combination with IFN-β (Figure S7). However, when LPS was combined with IFN-β, CXCL1 and CXCL2 production was modulated in WT but not *Ifnar1*$^{fl/fl}$ LysMCre macrophages, suggesting that the absence of IFNAR on myeloid cells can cause an enhanced chemokine response.

Microglia, the brain-endogenous macrophages, might also be targeted with LysMCre transgenic mice and could therefore also contribute to the IFN-mediated suppression of CNS autoimmunity. Indeed, by performing Southern-blot analysis, we observed a substantial deletion in hematopoietic microglia, whereas neuroectodermal astrocytes were devoid of homologous recombination in the presence of the Cre transgene (Figure 7A). Importantly, further in vivo examinations revealed that in the absence of IFNAR signaling, CD11b^{+}Ly-6^{lo}CD45^{lo} microglia were a major population within the CNS that expressed MHC class II molecules during EAE (Figure 7B). Moreover, *Ifnar1*$^{fl/fl}$ LysMCre microglia isolated from the CNS exhibited an altered CXCL2 production capacity in vitro upon LPS stimulation (Figure 7C), thereby potentially contributing to the phenotype observed.

Absence of a T Cell-Related Transcription Profile in Microglia upon IFN-β Challenge

To better understand how type 1 IFNs modulate the macrophage immune responses in general, we challenged microglia with IFN-β and investigated the IFN-induced transcriptional profiling. Cells were treated with IFN-β for 6 and 24 hr, and an Affymetrix Mouse Genome 430A 2.0 array was performed. The statistical

(left) and infiltration (right). Each symbol indicates mean of one mouse. Data are expressed as mean ± SEM. Significant differences are marked with asterisks.

(D) Enzyme-linked immunospot analysis of IFN-γ, IL-4, and IL-17 production by lymph node and CNS-derived MOG-reactive lymphocytes restimulated for 48 hr with MOG_{35-55}.

(E) Expression of chemokines at peak of disease (above) and Th1, Th2, and Th17 cell related factors during different disease stages (10, 18, and 30 days after immunization) (below) in the CNS of *Ifnar1*$^{-/-}$ (black symbols) or WT (white symbols) mice. Data are expressed as ratio of induced factors versus endogenous glyceraldehyde-3-phosphate dehydrogenase (GAPDH) and expressed as mean ± SEM. Significant differences are marked with asterisks.

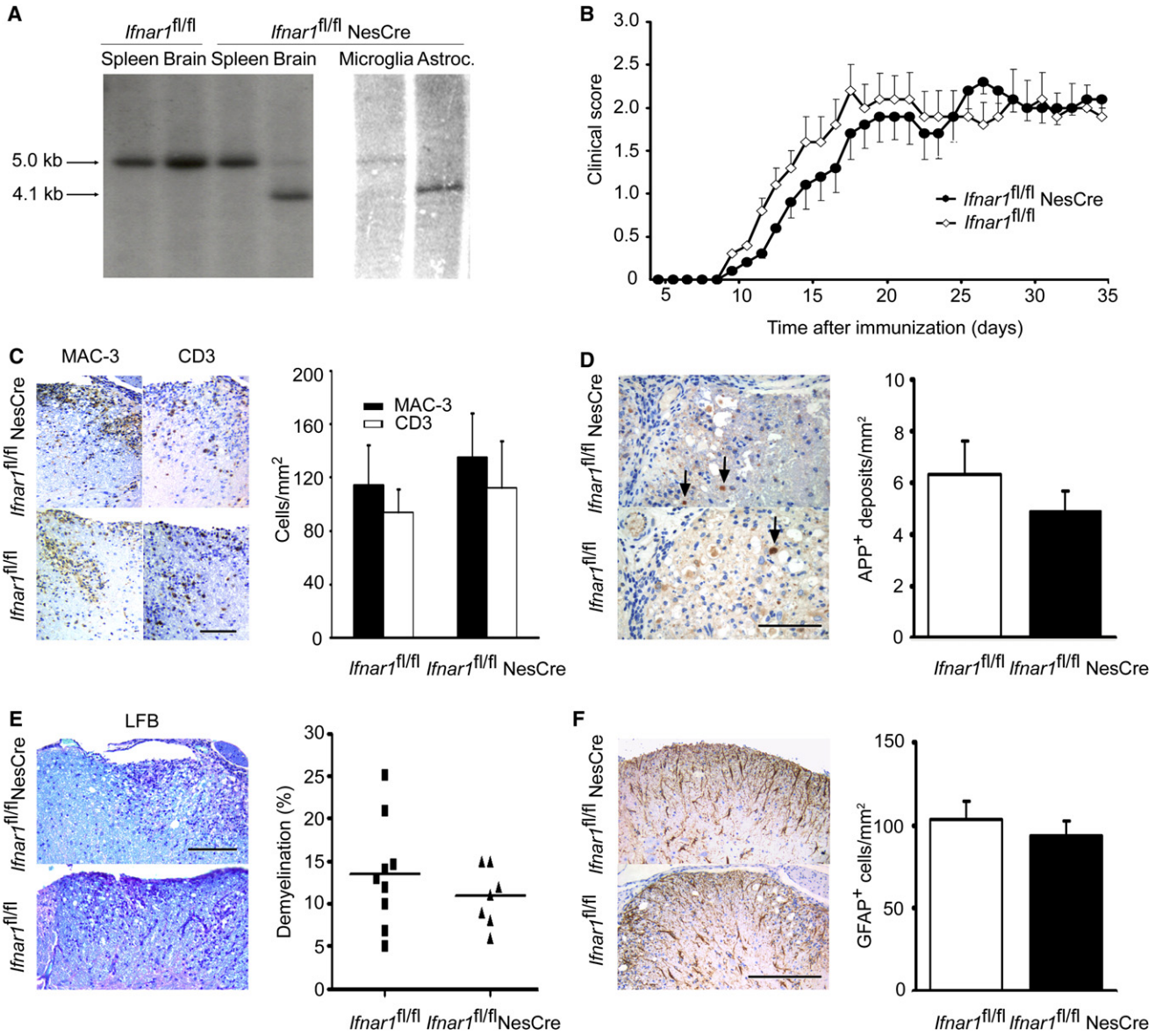

Figure 4. Brain-Specific IFNAR Expression Is Dispensable for the Autoimmune Process within the CNS

(A) Southern-blot analysis of different tissues from *Ifnar1*$^{fl/fl}$ NesCre mice. Deletion band (4.1 kb) and WT band (5.0 kb) are shown.

(B) Clinical course of EAE in *Ifnar1*$^{fl/fl}$ NesCre mice (filled circles) compared to the WT (open squares). One representative experiment out of two is shown.

(C) Histopathology of spinal cords visualized by MAC-3 for macrophages and by CD3 for T cells (left) and quantification thereof (right).

(D–F) CNS pathology in *Ifnar1*$^{fl/fl}$ NesCre animals. (D) shows distribution (left) and quantity (right) of amyloid precursor protein (APP) deposits representing axonal damage. (E) shows regions (left) and extent (right) of demyelination (luxol fast blue [LFB]). (F) shows the appearance and number of activated glial fibrillary acidic protein-positive (GFAP) astrocytes in the spinal cord during disease. Data are expressed as mean ± SEM ($n \geq 5$).

Scale bars represent 100 μm in (C)–(F).

procedures allowed the identification of 663 significantly regulated genes that were submitted to a k-means clustering analysis with R. This objective method allowed the detection of four different groups of gene induction with clusters 1, 2, and 4 that showed upregulated genes and cluster 3 with downregulated genes (Figure 7D).

We used the 533 upregulated genes from clusters 1, 2, and 4 for a functional analysis of overrepresentation of Gene Ontology terms in this genes by the GOstats package for R (Falcon and Gentleman, 2007). The most significant functional group of genes was found to lie within immune or host defense response rather than in the induction of Th1, Th2, or Th17 cell genes. Independent of the gene clusters discussed above, in Table S4, the most substantially upregulated genes after 6 or 24 hr are shown grouped according to their biological function. Most importantly, many chemokines, cytokines, costimulatory, antigen-presentation molecules, and macrophage-related activation markers were strongly upregulated, whereas no overt upregulation of genes indicative for a Th cell shift were detectable, suggesting a primary innate immune response of macrophages upon IFN-β challenge.

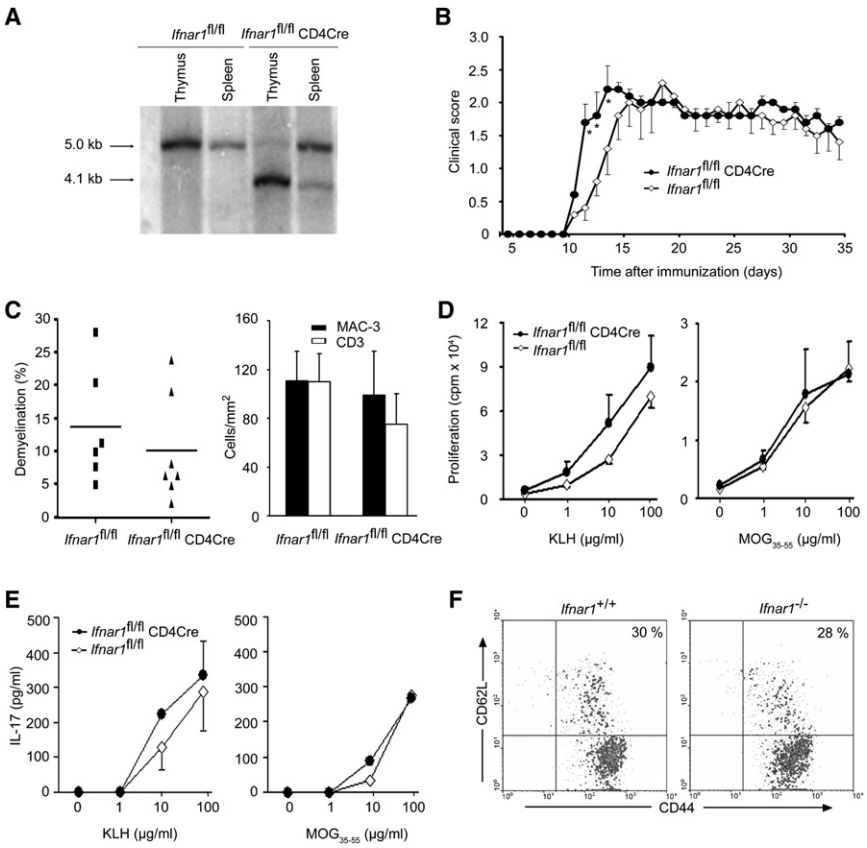

Figure 5. T Cell-Mediated IFNAR Signaling Is Not Required for the Effector Phase of EAE Disease

(A) Genomic Southern-blot analysis of several tissues from *Ifnar1*$^{fl/fl}$ CD4Cre animals.

(B) Disease course in *Ifnar1*$^{fl/fl}$ CD4Cre (filled circles) and WT mice (open squares). One representative experiment out of two is shown. Asterisks indicate statistical significance.

(C) Quantity of infiltrates at 35 days after immunization. Sections were stained with MAC-3 for macrophages and microglia, CD3 for lymphocytes, and luxol fast blue (LFB) for myelin. The scale bar represents 200 μm.

(D and E) Recall responses of *Ifnar1*$^{fl/fl}$ CD4Cre (filled circles) and WT (open squares) lymph node cells to either $MOG_{35–55}$ peptide or KLH at several dosages were measured by [H]thymidine-uptake (D) and IL-17 ELISA (E). Shown are representative of two independent experiments.

(F) Activation status of CNS-infiltrating T cells during autoimmune inflammation of the CNS (gated on CD4 cells).

Taken together, our data indicate that engagement of myeloid-specific IFNAR by endogenously produced IFN-β modulates the effector but not the priming phase of EAE and leads to aggravated autoimmunity by shaping the innate immune response of myeloid cells, e.g., cytokine and chemokine production, expression of surface immune receptors, and myelin phagocytosis.

DISCUSSION

We addressed here the function of the receptor of type I interferons (IFNAR) in an autoimmune inflammatory mouse model of MS where disease-associated IFN-β is produced locally in the CNS. By using gene-targeted mice, we were able to investigate the role of ubiquitously expressed IFNAR specifically on brain cells as well as on other cell types that participate in EAE pathogenesis, including T and B lymphocytes as well as macrophages and granulocytes. This approach allowed us to identify in vivo the main cell type targeted by interferon action that essentially contributes to CNS autoimmunity.

We found that IFN-β is produced locally in the CNS, but not in the blood, during inflammatory demyelination and that IFNAR-dependent genes show disease-associated upregulation. Although many cell types are capable of producing type 1 interferons during infection and autoimmunity, the main producers are thought to be plasmacytoid dendritic cells in the blood (Asselin-Paturel et al., 2001; Ito et al., 2006). However, brain-endogenous cells, e.g., microglia, astrocytes, and neurons, have been shown to produce IFN-β as well (Delhaye et al., 2006; Town et al., 2006). It has been described that plasmacytoid DCs, conventional DCs, and CD8 alpha^{+} DCs do invade during acute relapsing EAE induced by a proteolipid protein peptide of amino acids 178–191 (Miller et al., 2007). Nevertheless, the cellular source of disease associated IFN-β production within in the CNS remains to be determined in our $MOG_{35–55}$ EAE model.

In order to test the functional significance of the IFNAR system in the EAE model, we immunized mice lacking IFNAR from all tissues. Importantly, these mice showed an intensified effector phase with increased rate of lethality accompanied by aggravated neuropathological changes, consisting of elevated numbers of invading macrophages and stronger demyelination. Despite higher local production of chemoattractants within the CNS, the number of infiltrating mononuclear cells in the preclinical phase and the ratio of Th cell cytokines remained unchanged. Some results are consistent with a previous observation that mice lacking one ligand of IFNAR, namely IFN-β, developed a more severe $MBP_{89–101}$-induced EAE (Teige et al., 2003), but in contrast to these earlier findings, we could not detect a substantial increase of the Th1 cell cytokine IFN-γ within the CNS of affected mice. Further, our results from the transfer EAE experiments revealed that antigen-restimulated T cells from WT mice induced significantly more disease in IFNAR-deficient animals, indicating that IFNAR expression on host-derived cells is critical for disease induction.

We applied the Cre-LoxP technique to identify the pathogenic role of neuroectoderm-derived CNS host cells, namely astrocytes, oligodendrocytes, and neurons, during EAE. Although it has been shown that astrocytes and oligodendrocytes have proinflammatory properties under several conditions (van Loo et al., 2006), our results strongly indicate that brain-restricted IFNAR expression does not contribute to the pathogenesis of EAE. Our data are unexpected because previous reports pointed

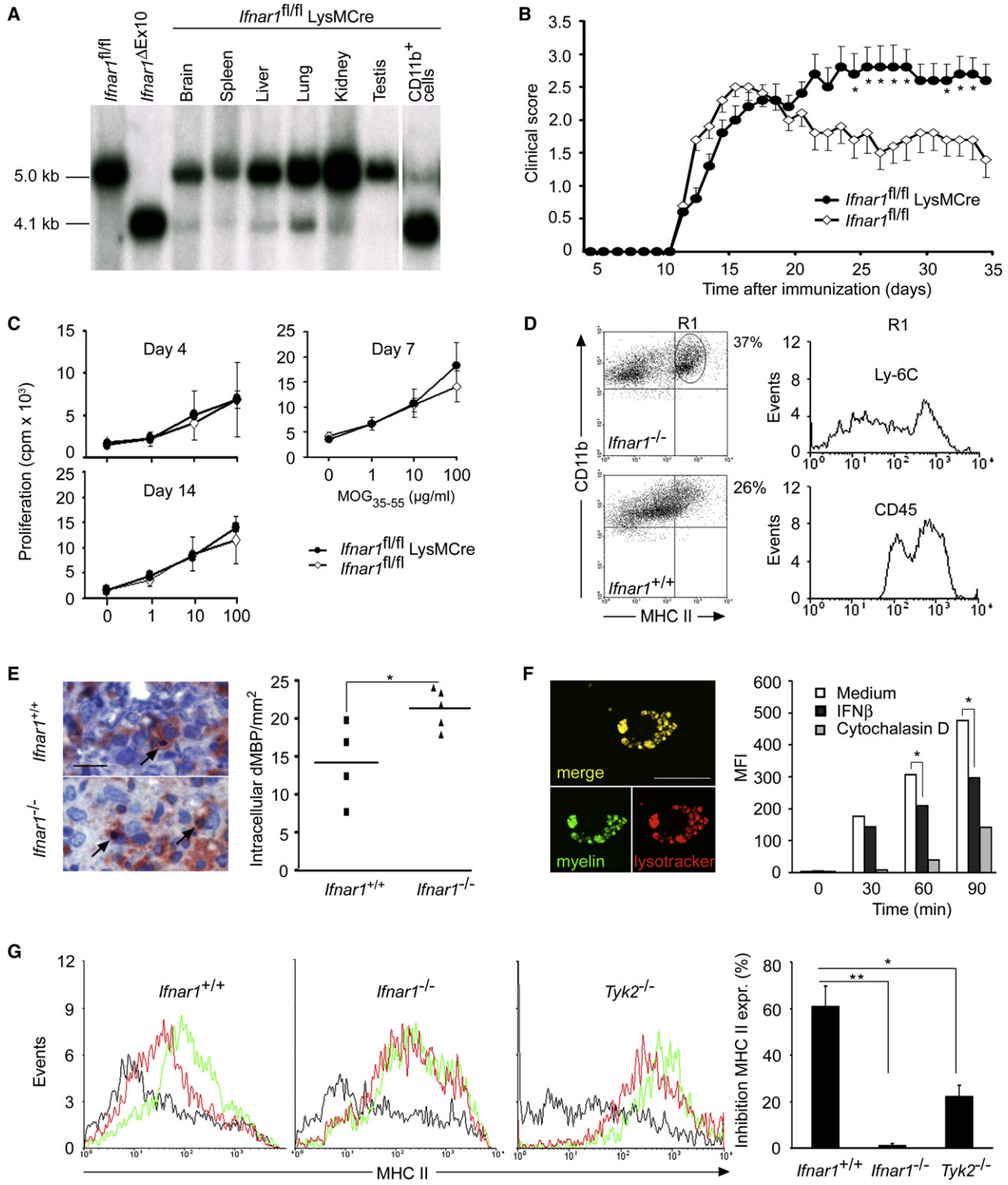

Figure 6. IFNAR Signaling on Peripheral Myeloid Cells Regulates Effector Phase of Autoimmune Encephalomyelitis by Limiting Cell Activation

(A) Tissue-restricted deletion of the floxed IFNAR locus is shown by Southern-blot analysis in *Ifnar1*$^{fl/fl}$ LysMCre mice. MACS-sorted splenic CD11b^{+} cells were used as positive control. Deletion band (4.1 kb) and WT band (5.0 kb) are shown.

(B) Disease course in the absence of IFNAR on macrophages and neutrophiles. Statistically significant time points are marked with asterisks ($p < 0.05$). The results are representative of five independent experiments.

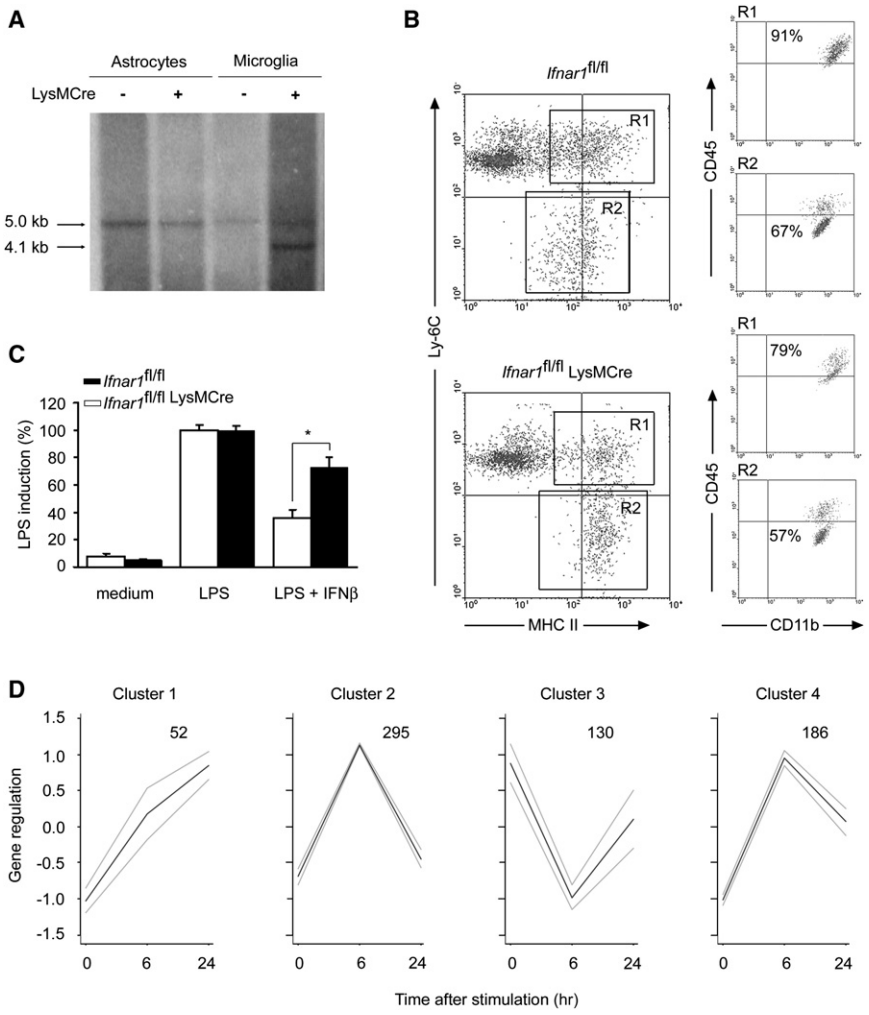

Figure 7. CNS-Endogenous Microglia Have a Changed Immune Pattern in the Absence of IFNAR during EAE

(A) Southern-blot analysis of *Ifnar1*$^{fl/fl}$ LysMCre microglia and astrocytes. Deletion band (4.1 kb) and WT band (5.0 kb) are shown.

(B) FACS of MHC class II molecules on CD11b^{+}Ly-6C^{lo}CD45^{lo} microglia in the CNS of diseased animals.

(C) CXCL2 production of IFNAR-deficient microglia (*Ifnar1*$^{fl/fl}$ LysMCre, white bars) and negative littermates (black bars) upon costimulation with LPS and IFN-β. Data represent mean ± SEM ($n \geq 6$).

(D) Gene induction pattern of all 663 significantly regulated genes after IFN-β challenge in microglia with a k-means cluster analysis to identify specific cohorts of gene induction. Clusters are defined by different gene regulation over time. Numbers indicate the quantity of regulated genes within the respective cluster.

toward a modulating role of IFN-β on astrocytes (Okada et al., 2005; Teige et al., 2006) and oligodendrocytes (Passaquin et al., 1989; Mastronardi et al., 2004). Despite the fact that our results clearly rule out a disease-modulating role for IFNAR on neuroectodermal cells during EAE, it is still possible that this IFNAR expression might be more important in chronic relapsing EAE models.

EAE is a T cell-mediated disease, and it has been reported that IFNAR is expressed on lymphocytes, as well (Pogue et al., 2004). However, in our study, T cell-restricted *Ifnar1*$^{-/-}$ mice developed a similar course of EAE with comparable neuropathological changes. Furthermore, we could not detect any differences in the effector function of T cells because MOG_{35-55}-specific T lymphocytes produced equivalent amounts of IFN-γ, IL-17, and IL-4 and proliferated similarly in the absence of IFNAR. In addition, surface expression of activation markers CD62L and CD44 of brain infiltrating T lymphocytes was not influenced by the absence or presence of IFNAR. Hence, our findings do not support the idea that endogenously produced IFN-β acts beneficially on T cells, either through inhibiting T cell proliferation or through skewing the T cell-cytokine response.

The immune-modulatory function of B cells has been described in the context of EAE, and it is feasible that type I IFNs modulate their regulatory function (Fillatreau et al., 2002). Yet, our analysis of B cell-restricted *Ifnar1*$^{-/-}$ mice revealed an unaltered course of disease with normal infiltrates and typical demyelination, thus disproving a functional role of IFNAR on B cells for the pathogenesis of EAE. The absence of IFNAR on B cells does not affected MOG-specific IL-10 production by B cells, showing again the normal B cell function in IFNAR-deficient mice.

In order to test the hypothesis that IFNAR engagement on myeloid cells is crucial in modulating CNS autoimmunity, we took advantage of the LysM Cre transgenic mouse. Notably, the

(C) Priming of MOG-specific T lymphocytes at different time points of disease in lymph nodes of *Ifnar1*$^{fl/fl}$ LysMCre (filled circles) or WT (open symbols) mice. cpm indicates counts per minute. Data represent mean ± SEM.

(D) Characterization of CNS-infiltrating CD11b^{+} MHC class II^{+} myeloid cells (left) during peak of disease in *Ifnar1*$^{-/-}$ mice. These cells exhibited Ly-6C^{hi} and Ly-6C^{lo} and CD45^{hi} and CD45^{lo} expression patterns.

(E) Accumulation of degraded myelin protein (dMBP, black arrows) in MAC-3^{+} macrophages (red) in the absence of IFNAR (left) and quantification thereof (right) in EAE diseased CNS tissue. Significant differences are marked with an asterisk. The scale bar represents 15 μm.

(F) Modulation of myelin uptake by IFN-β. Macrophages ingested fluorescein isothiocyanate (FITC)-labeled myelin (green) in lysosomal compartments (red, left panel). Myelin uptake in the presence of external IFN-β (black bars) or cytochalasin D (gray bars, right panel) is shown. One experiment out of four is shown. Significant differences are marked with asterisks. The scale bar represents 5 μm.

(G) Aberrant MHC class II regulation on cultured peritoneal *Ifnar1*$^{-/-}$ macrophages in the absence of Tyk2. Cells were stimulated with either IFN-β (black lines) or IFN-γ (green lines) alone or combination of both (red lines). Inhibition of IFN-γ-induced MHC II production by IFN-β in WT, IFNAR$^{-/-}$, and *Tyk2*$^{-/-}$ cells (right). **: $p < 0.01$, *: $p < 0.05$.

course of EAE in macrophage- and neutrophil-specific *Ifnar1*$^{-/-}$ mice was strongly increased during the effector phase, and some mice even died because of severe disease. The clinical differences to control mice, however, were not always statistically relevant, as seen in the total *Ifnar1*$^{-/-}$ situation, most likely due to the fact that gene deletion in myeloid cells is incomplete (Grivennikov et al., 2005). Which myeloid cell types are crucial in the IFNAR-mediated change of CNS autoimmunity? Although granulocytes have been shown to have immunoregulatory capacity during EAE development (Zehntner et al., 2005), their number was, in contrast to MAC-3^{+} mononuclear phagocytes, quite low and not elevated in the CNS (data not shown). The MAC-3 antigen can be found on tissue macrophages, thioglycollate-elicited peritoneal macrophages, and monocytes (Walker et al., 1985), suggesting that these cells might shape the immmune response within in the CNS. Both CD11b^{+}Ly-6C^{hi} and CD11b^{+}Ly-6C^{lo} monocytes were found to be targeted by the LysM Cre transgene, and therefore these cells might task as endogenous type I interferon-dependent modulators of CNS autoimmunity from the peripheral site. Importantly, professional antigen-presenting cells (APCs) such as plasmacytoid DCs or myeloid DCs were not targeted by the LysM Cre transgene, disproving a role of IFNAR on these cell subsets during sterile autoimmunity of the CNS.

Microglia cells are another possible candidate that could suppress inflammatory demyelination in a type I-interferon-dependent manner. They are the brain-endogenous macrophages and populate the CNS early during development to form a regularly spaced network of ramified cells (Priller et al., 2001). Microglia become rapidly activated in most pathological conditions of the CNS. In autoimmune diseases such as multiple sclerosis, most experimental results point to a detrimental role of microglia; for example, then can produce neurotoxic molecules, proinflammatory cytokines, and chemokines and can present self-antigens (Steinman, 1996). How could type I interferons modulate microglia-mediated damage in EAE? Nitric oxide (NO) and its adducts may disrupt CNS tissue integrity (Steinman et al., 2002), whereas microglia-derived cytokines and chemokines such as TNF and CXCL2 activate and attract blood-derived leukocytes. These may in turn interfere with CNS homeostasis (e.g., by damaging myelin) (Steinman et al., 2002; Hanisch, 2002). However, effects of IFN-β on production of proinflammatory mediators, such as TNFα, IL-1, or NO, are controversial and seem to be dependent on the mode and conditions of activation (Jin et al., 2007). Further, reactivation of myelin-specific T cells within the CNS upon recognition of local autoantigens is critical to induce and/or sustain EAE. But it is still debated whether and to what extent microglia present myelin-associated antigens to autoreactive T cells in vivo (Ford et al., 1995). In vitro, however, it has been demonstrated that IFN-β exerts its beneficial effects also by reducing the antigen-presenting capacity of CNS-specific APCs such as microglia, which in turn inhibits the effector functions of encephalitogenic T cells (Teige et al., 2006). Interestingly, the lack of IFNAR on CD11b^{+} myeloid cells did not changed the Th cell polarization of T cells in our settings, suggesting that other mechanisms apart from antigen presentation might be vital.

Thus, monocytes and macrophages and their brain-specific equivalent, the microglia, are the IFNAR-dependent myeloid cells critical in shaping CNS autoimmunity. IFNAR signaling in these cells potentially modulates, for example, their activation state. We found a clear increase of MHC class II molecules in the absence of IFNAR, indicating hyperactivation of these cells. These data are in line with previous reports describing a role of IFN-β for MHC class II expression on monocytes in vitro (Kato et al., 1992; Li et al., 1998).

Our data might provide unique insights into disease-limiting mechanisms of autoimmune inflammation, which might open new avenues toward more cell-specific IFN-β-based therapies that probably would reduce the severity of side effects.

EXPERIMENTAL PROCEDURES

Mice

Ifnar1$^{-/-}$ mice (Muller et al., 1994) originally provided by R. M. Zinkernagel (Zurich, Switzerland) were backcrossed 20 times to C57BL/6. Mice carrying loxP-flanked IFNAR (Kamphuis et al., 2006) were crossed with transgenic mice expressing Cre recombinase under the control of the nestin (Tronche et al., 1999), CD4 (Wolfer et al., 2001), CD19 (Rickert et al., 1997), or LysM (Clausen et al., 1999) promoter, each backcrossed at least ten times to C57BL/6. All mice were bred in house under pathogen-free conditions.

Induction of EAE

Female 6- to 10-week-old mice from each group were immunized subcutaneously with 200 μg of $MOG_{35–55}$ peptide emulsified in CFA containing 1 mg of Mycobacterium tuberculosis (H37RA; Difco Laboratories, Detroit, MI). The mice received intraperitonal injections with 250 ng pertussis toxin (Sigma-Aldrich, Deisenhofen, Germany) at the time of immunization and 48 hr later. Adoptive transfer was performed as described (Becher et al., 2001; Prinz et al., 2006). All animal experiments have been approved by the ethics review board for animal studies at the University of Göttingen.

Clinical Evaluation

Mice were scored daily as follows: 0, no detectable signs of EAE; 0.5, distal limb tail; 1.0, complete limb tail; 1.5, limb tail and hind-limb weakness; 2, unilateral partial hind-limb paralysis; 2.5, bilateral partial hind-limb paralysis; 3, complete bilateral hind-limb paralysis; 3.5, complete hind-limb paralysis and unilateral forelimb paralysis; 4, total paralysis of forelimbs and hind limbs; and 5, death.

Histology

Mice were sacrificed with CO_2. Histology was performed as described recently (Prinz et al., 2006; van Loo et al., 2006). Spinal cords were removed and fixed in 4% buffered fomalin. Then, spinal cords were dissected and embedded in paraffin before staining with hematoxylin eosin (H&E) or luxol fast blue (LFB) to assess the degree of demyelination, MAC-3 (BD PharMingen) for macrophages and microglia, CD3 for T cells (Serotec, Düsseldorf, Germany), APP for amyloid precursor protein (Chemicon, Temecula, CA), chloracetate esterase for polymorphonuclear granulocytes (Sigma-Aldrich, Munich Germany), dMPB for degraded myelin basic protein (Chemicon, Temecula, CA), and GFAP for astrocytes (Dako, Hamburg, Germany).

RNA

Spinal cord tissue was freshly isolated and RNA isolated with TRI-Reagent (Sigma) according to the manufacturer's protocol. RNA (10 μg/lane) was separated on 1% formaldehyde-agarose gels and blotted to positively charged nylon membrane. Probes were radioactively labeled with Rediprime (Amersham) and hybridized with Express-Hyb-Solution (Clontech) according to the manufacturer's protocol.

Flow Cytometry

The cells were stained with primary antibodies directed against Ly-6C, CD45, CD44, MAR1-5A3, CD62L, MHC class II, CD11b, CD4, P-STAT-1, and B220 for 30 min at 4°C. The cells were washed and analyzed with a FACSCalibur (Becton Dickinson). Viable cells were gated by forward and side scatter of light. Data were acquired with CellQuest software (Becton Dickinson).

Postacquisition analysis was perfomed with WinMDI 2.8 software (Scripps-Research Institute).

Recall Responses, B Cell Activation Assay, IFN-β Measurements, and ELISPOT Analysis

Recall assays were performed as described recently (Prinz et al., 2006). For cytokine analysis, sister cultures were harvested 4 hr after culture supernatants were analyzed by ELISA for IFN-γ and IL-17 (R&D Systems, Bergisch-Gladbach, Germany).

Spinal cord homogenates were prepared and diluted 1:5 in lysis buffer as described by us (Prinz and Hanisch, 1999), and IFN-β levels were measured by application of an IFN-β ELISA according to the instructions (PBL Biomedical Laboratories, New Brunswick, NJ). B cell activation was determined as described recently by Fillatreau (Fillatreau et al., 2002). Enzyme-linked immunospot analysis was performed as reported previously by us (Gutcher et al., 2006).

Peritoneal Macrophages, Microglia, and Stimulation

Mice were injected with thioglycolate (29 g/l phosphate-buffered saline [PBS]) intraperitoneally (i.p.). Peritoneal cells were collected 96 hr after injection by lavage of the peritoneal cavity with 2 ml of ice-cold PBS. Cells were plated in cell-culture plates and nonadhering cells were removed by washing of the wells 1 hr later. Microglia were prepared as described (Prinz and Hanisch, 1999). Macrophages and microglia were incubated for 24 hr prior to experiments and stimulated with LPS (10 ng/ml), IFN-β (10 ng/ml), and TNFα (10 ng/ml) for 18 hr. Protein levels were detected by ELISA as described by the manufacturer (R&D Systems, Bergisch-Gladbach).

Real-Time PCR and Microarray Analysis

RNA was extracted from tissues and flushed with ice-cold HBSS, and RNA was isolated with RNAeasy Mini kits (QIAGEN, Hilden, Germany) according to the manufacturer's instructions. The samples were treated with DNaseI (Roche, Mannheim, Germany), and 1 μg of RNA was transcribed into complementary DNA (cDNA) with oligo-dT primers and the SuperScript II RT kit (Invitrogen, Carlsbad, CA). cDNA (2.5 μl) was transferred into a 96-well Multiply PCR-plate (Sarstedt, Germany), and 12.5 μl ABsolute QPCR SYBR Green master mix (ABgene, Surrey, UK) plus 19.6 μl ddH_2O was added. The PCR reaction was performed as described recently (Prinz et al., 2006; Mildner et al., 2007).

Total RNA (1 μg) was processed with the MessageAmp II-Biotion Enhanced Kit (Ambion) and hybridized to the murine array 430 A2.0 according to the manufacturer's protocols (Affymetrix). Microarrays were scanned and initially analyzed with Affymetrix GCOS software. Two biological replicates per condition (0 hr, 6 hr, and 24 hr IFN-β) were carried out. CEL files were processed for global normalization, and expression values were generated with the robust multichip average (rma) algorithm in the R affy package (Bolstad et al., 2003). So that differential expression could be tested for, the bayesian-adjusted t statistics from the linear models for Microarray data (limma) package with subsequent multiple testing correction based on Benjamini-Hochberg was used (Hochberg and Benjamini, 1990). Probe sets were considered to be differentially expressed if there was a minimum n-fold change of 3 between any of the three conditions and the p value for 6 hr or 24 hr was below 0.01.

SUPPLEMENTAL DATA

Seven figures, four tables, and two movies are available at http://www.immunity.com/cgi/content/full/28/5/675/DC1/.

ACKNOWLEDGMENTS

We thank O. Kowatsch, D. Kreuz, and E. Pralle for excellent technical assistance. We are grateful to R.D. Schreiber, St. Louis, for generous supply of the MAR1-5A3 antibody and to T. Decker, Vienna, for Tyk-2-deficient mice. Gemeinnützige Hertie-Stiftung supported M.P. German Research Council (DFG, SFB432, B15) and the Volkswagen Foundation supported U.K. This work was supported by generous research grants from Biogen Idec and Merck Serono to M.P. H.S. and A.M. are fellows of the Gertrud Reemtsma foundation.

Received: October 9, 2007
Revised: January 27, 2008
Accepted: March 4, 2008
Published online: April 17, 2008

REFERENCES

Asselin-Paturel, C., Boonstra, A., Dalod, M., Durand, I., Yessaad, N., Dezutter-Dambuyant, C., Vicari, A., O'Garra, A., Biron, C., Briere, F., et al. (2001). Mouse type I IFN-producing cells are immature APCs with plasmacytoid morphology. Nat. Immunol. *2*, 1144–1150.

Becher, B., Durell, B.G., Miga, A.V., Hickey, W.F., and Noelle, R.J. (2001). The clinical course of experimental autoimmune encephalomyelitis and inflammation is controlled by the expression of CD40 within the central nervous system. J. Exp. Med. *193*, 967–974.

Bolstad, B.M., Irizarry, R.A., Astrand, M., and Speed, T.P. (2003). A comparison of normalization methods for high density oligonucleotide array data based on variance and bias. Bioinformatics *19*, 185–193.

Brod, S.A., and Burns, D.K. (1994). Suppression of relapsing experimental autoimmune encephalomyelitis in the SJL/J mouse by oral administration of type I interferons. Neurology *44*, 1144–1148.

Brod, S.A., and Khan, M. (1996). Oral administration of IFN-alpha is superior to subcutaneous administration of IFN-alpha in the suppression of chronic relapsing experimental autoimmune encephalomyelitis. J. Autoimmun. *9*, 11–20.

Clausen, B.E., Burkhardt, C., Reith, W., Renkawitz, R., and Forster, I. (1999). Conditional gene targeting in macrophages and granulocytes using LysMcre mice. Transgenic Res. *8*, 265–277.

Delhaye, S., Paul, S., Blakqori, G., Minet, M., Weber, F., Staeheli, P., and Michiels, T. (2006). Neurons produce type I interferon during viral encephalitis. Proc. Natl. Acad. Sci. USA *103*, 7835–7840.

Falcon, S., and Gentleman, R. (2007). Using GOstats to test gene lists for GO term association. Bioinformatics *23*, 257–258.

Fillatreau, S., Sweenie, C.H., McGeachy, M.J., Gray, D., and Anderton, S.M. (2002). B cells regulate autoimmunity by provision of IL-10. Nat. Immunol. *3*, 944–950.

Floris, S., Ruuls, S.R., Wierinckx, A., van der Pol, S.M., Dopp, E., van der Meide, P.H., Dijkstra, C.D., and De Vries, H.E. (2002). Interferon-beta directly influences monocyte infiltration into the central nervous system. J. Neuroimmunol. *127*, 69–79.

Ford, A.L., Goodsall, A.L., Hickey, W.F., and Sedgwick, J.D. (1995). Normal adult ramified microglia separated from other central nervous system macrophages by flow cytometric sorting. Phenotypic differences defined and direct ex vivo antigen presentation to myelin basic protein-reactive CD4+ T cells compared. J. Immunol. *154*, 4309–4321.

Frohman, E.M., Racke, M.K., and Raine, C.S. (2006). Multiple sclerosis–the plaque and its pathogenesis. N. Engl. J. Med. *354*, 942–955.

Gold, R., Linington, C., and Lassmann, H. (2006). Understanding pathogenesis and therapy of multiple sclerosis via animal models: 70 years of merits and culprits in experimental autoimmune encephalomyelitis research. Brain *129*, 1953–1971.

Grivennikov, S.I., Tumanov, A.V., Liepinsh, D.J., Kruglov, A.A., Marakusha, B.I., Shakhov, A.N., Murakami, T., Drutskaya, L.N., Forster, I., Clausen, B.E., et al. (2005). Distinct and nonredundant in vivo functions of TNF produced by t cells and macrophages/neutrophils: Protective and deleterious effects. Immunity *22*, 93–104.

Gutcher, I., Urich, E., Wolter, K., Prinz, M., and Becher, B. (2006). Interleukin 18-independent engagement of interleukin 18 receptor-alpha is required for autoimmune inflammation. Nat. Immunol. *7*, 946–953.

Hanisch, U.K. (2002). Microglia as a source and target of cytokines. Glia *40*, 140–155.

Heine, S., Ebnet, J., Maysami, S., and Stangel, M. (2006). Effects of interferon-beta on oligodendroglial cells. J. Neuroimmunol. *177*, 173–180.

Hochberg, Y., and Benjamini, Y. (1990). More powerful procedures for multiple significance testing. Stat. Med. *9*, 811–818.

Ito, T., Kanzler, H., Duramad, O., Cao, W., and Liu, Y.J. (2006). Specialization, kinetics, and repertoire of type 1 interferon responses by human plasmacytoid predendritic cells. Blood *107*, 2423–2431.

Jin, S., Kawanokuchi, J., Mizuno, T., Wang, J., Sonobe, Y., Takeuchi, H., and Suzumura, A. (2007). Interferon-beta is neuroprotective against the toxicity induced by activated microglia. Brain Res. *1179*, 140–146.

Kamphuis, E., Junt, T., Waibler, Z., Forster, R., and Kalinke, U. (2006). Type I interferons directly regulate lymphocyte recirculation and cause transient blood lymphopenia. Blood *108*, 3253–3261.

Kato, T., Kitaura, M., Inaba, K., Watanabe, Y., Kawade, Y., and Muramatsu, S. (1992). Suppression of macrophage Ia antigen expression by endogenous interferon-alpha/beta. J. Interferon Res. *Spec No*, 29–41.

Kozovska, M.E., Hong, J., Zang, Y.C., Li, S., Rivera, V.M., Killian, J.M., and Zhang, J.Z. (1999). Interferon beta induces T-helper 2 immune deviation in MS. Neurology *53*, 1692–1697.

Li, Q., Milo, R., Panitch, H., and Bever, C.T., Jr. (1998). Effect of propranolol and IFN-beta on the induction of MHC class II expression and cytokine production by IFN-gamma IN THP-1 human monocytic cells. Immunopharmacol. Immunotoxicol. *20*, 39–61.

Mastronardi, F.G., Min, W., Wang, H., Winer, S., Dosch, M., Boggs, J.M., and Moscarello, M.A. (2004). Attenuation of experimental autoimmune encephalomyelitis and nonimmune demyelination by IFN-beta plus vitamin B12: Treatment to modify notch-1/sonic hedgehog balance. J. Immunol. *172*, 6418–6426.

McRae, B.L., Semnani, R.T., Hayes, M.P., and van Seventer, G.A. (1998). Type I IFNs inhibit human dendritic cell IL-12 production and Th1 cell development. J. Immunol. *160*, 4298–4304.

Mildner, A., Schmidt, H., Nitsche, M., Merkler, D., Hanisch, U.K., Mack, M., Heikenwalder, M., Bruck, W., Priller, J., and Prinz, M. (2007). Microglia in the adult brain arise from Ly-6C(hi)CCR2(+) monocytes only under defined host conditions. Nat. Neurosci. *10*, 1544–1553.

Miller, S.D., McMahon, E.J., Schreiner, B., and Bailey, S.L. (2007). Antigen presentation in the CNS by myeloid dendritic cells drives progression of relapsing experimental autoimmune encephalomyelitis. Ann. N Y Acad. Sci. *1103*, 179–191.

Muller, U., Steinhoff, U., Reis, L.F., Hemmi, S., Pavlovic, J., Zinkernagel, R.M., and Aguet, M. (1994). Functional role of type I and type II interferons in antiviral defense. Science *264*, 1918–1921.

Neilley, L.K., Goodin, D.S., Goodkin, D.E., and Hauser, S.L. (1996). Side effect profile of interferon beta-1b in MS: Results of an open label trial. Neurology *46*, 552–554.

Okada, K., Kuroda, E., Yoshida, Y., Yamashita, U., Suzumura, A., and Tsuji, S. (2005). Effects of interferon-beta on the cytokine production of astrocytes. J. Neuroimmunol. *159*, 48–54.

Owens, T., Wekerle, H., and Antel, J. (2001). Genetic models for CNS inflammation. Nat. Med. *7*, 161–166.

Panitch, H.S., Hirsch, R.L., Schindler, J., and Johnson, K.P. (1987). Treatment of multiple sclerosis with gamma interferon: Exacerbations associated with activation of the immune system. Neurology *37*, 1097–1102.

Passaquin, A.C., Coupin, G., Schreier, W.A., Poindron, P., Cole, R.A., and de Vellis, J. (1989). Interferon inhibits the accumulation of glycerol phosphate dehydrogenase mRNA in oligodendrocytes and C6 cells. Neurochem. Res. *14*, 987–993.

Pogue, S.L., Preston, B.T., Stalder, J., Bebbington, C.R., and Cardarelli, P.M. (2004). The receptor for type I IFNs is highly expressed on peripheral blood B cells and monocytes and mediates a distinct profile of differentiation and activation of these cells. J. Interferon Cytokine Res. *24*, 131–139.

Priller, J., Flügel, A., Wehner, T., Boentert, M., Haas, C.A., Prinz, M., Fernandez-Klett, F., Prass, K., Bechmann, I., de Boer, B.A., et al. (2001). Targeting gene-modified hematopoietic cells to the central nervous system: Use of green fluorescent protein uncovers microglial engraftment. Nat. Med. *7*, 1356–1361.

Prinz, M., and Hanisch, U.K. (1999). Murine microglial cells produce and respond to interleukin-18. J. Neurochem. *72*, 2215–2218.

Prinz, M., Garbe, F., Schmidt, H., Mildner, A., Gutcher, I., Wolter, K., Piesche, M., Schroers, R., Weiss, E., Kirschning, C.J., et al. (2006). Innate immunity mediated by TLR9 modulates pathogenicity in an animal model of multiple sclerosis. J. Clin. Invest. *116*, 456–464.

Rickert, R.C., Roes, J., and Rajewsky, K. (1997). B lymphocyte-specific, Cre-mediated mutagenesis in mice. Nucleic Acids Res. *25*, 1317–1318.

Satoh, J., Paty, D.W., and Kim, S.U. (1995). Differential effects of beta and gamma interferons on expression of major histocompatibility complex antigens and intercellular adhesion molecule-1 in cultured fetal human astrocytes. Neurology *45*, 367–373.

Satoh, J., Nanri, Y., Tabunoki, H., and Yamamura, T. (2006). Microarray analysis identifies a set of CXCR3 and CCR2 ligand chemokines as early IFN-beta-responsive genes in peripheral blood lymphocytes in vitro: An implication for IFNbeta-related adverse effects in multiple sclerosis. BMC Neurol. *6*, 18.

Steinman, L. (1996). Multiple sclerosis: A coordinated immunological attack against myelin in the central nervous system. Cell *85*, 299–302.

Steinman, L. (2007). A brief history of T(H)17, the first major revision in the T(H)1/T(H)2 hypothesis of T cell-mediated tissue damage. Nat. Med. *13*, 139–145.

Steinman, L., Martin, R., Bernard, C., Conlon, P., and Oksenberg, J.R. (2002). Multiple sclerosis: Deeper understanding of its pathogenesis reveals new targets for therapy. Annu. Rev. Neurosci. *25*, 491–505.

Stone, L.A., Frank, J.A., Albert, P.S., Bash, C., Smith, M.E., Maloni, H., and McFarland, H.F. (1995). The effect of interferon-beta on blood-brain barrier disruptions demonstrated by contrast-enhanced magnetic resonance imaging in relapsing-remitting multiple sclerosis. Ann. Neurol. *37*, 611–619.

Teige, I., Treschow, A., Teige, A., Mattsson, R., Navikas, V., Leanderson, T., Holmdahl, R., and Issazadeh-Navikas, S. (2003). IFN-beta gene deletion leads to augmented and chronic demyelinating experimental autoimmune encephalomyelitis. J. Immunol. *170*, 4776–4784.

Teige, I., Liu, Y., and Issazadeh-Navikas, S. (2006). IFN-beta inhibits T cell activation capacity of central nervous system APCs. J. Immunol. *177*, 3542–3553.

Town, T., Jeng, D., Alexopoulou, L., Tan, J., and Flavell, R.A. (2006). Microglia recognize double-stranded RNA via TLR3. J. Immunol. *176*, 3804–3812.

Tronche, F., Kellendonk, C., Kretz, O., Gass, P., Anlag, K., Orban, P.C., Bock, R., Klein, R., and Schutz, G. (1999). Disruption of the glucocorticoid receptor gene in the nervous system results in reduced anxiety. Nat. Genet. *23*, 99–103.

van Loo, G., De Lorenzi, R., Schmidt, H., Huth, M., Mildner, A., Schmidt-Supprian, M., Lassmann, H., Prinz, M.R., and Pasparakis, M. (2006). Inhibition of transcription factor NF-kappaB in the central nervous system ameliorates autoimmune encephalomyelitis in mice. Nat. Immunol. *7*, 954–961.

Walker, E.B., Akporiaye, E.T., Warner, N.L., and Stewart, C.C. (1985). Characterization of subsets of bone marrow-derived macrophages by flow cytometry analysis. J. Leukoc. Biol. *37*, 121–136.

Wandinger, K.P., Sturzebecher, C.S., Bielekova, B., Detore, G., Rosenwald, A., Staudt, L.M., McFarland, H.F., and Martin, R. (2001). Complex immunomodulatory effects of interferon-beta in multiple sclerosis include the upregulation of T helper 1-associated marker genes. Ann. Neurol. *50*, 349–357.

Waubant, E., Vukusic, S., Gignoux, L., Dubief, F.D., Achiti, I., Blanc, S., Renoux, C., and Confavreux, C. (2003). Clinical characteristics of responders to interferon therapy for relapsing MS. Neurology *61*, 184–189.

Wolfer, A., Bakker, T., Wilson, A., Nicolas, M., Ioannidis, V., Littman, D.R., Lee, P.P., Wilson, C.B., Held, W., MacDonald, H.R., et al. (2001). Inactivation of Notch 1 in immature thymocytes does not perturb CD4 or CD8T cell development. Nat. Immunol. *2*, 235–241.

Zehntner, S.P., Brickman, C., Bourbonniere, L., Remington, L., Caruso, M., and Owens, T. (2005). Neutrophils that infiltrate the central nervous system regulate T cell responses. J. Immunol. *174*, 5124–5131.

Supplemental Data

Distinct and Nonredundant In Vivo Functions of IFNAR on Myeloid Cells Limit Autoimmunity in the Central Nervous System

Marco Prinz, Hauke Schmidt, Alexander Mildner, Klaus-Peter Knobeloch, Uwe-Karsten Hanisch, Jenni Raasch, Doron Merkler, Claudia Detje, Ilona Gutcher, Jörg Mages, Roland Lang, Roland Martin, Ralf Gold, Burkhard Becher, Wolfgang Brück, and Ulrich Kalinke

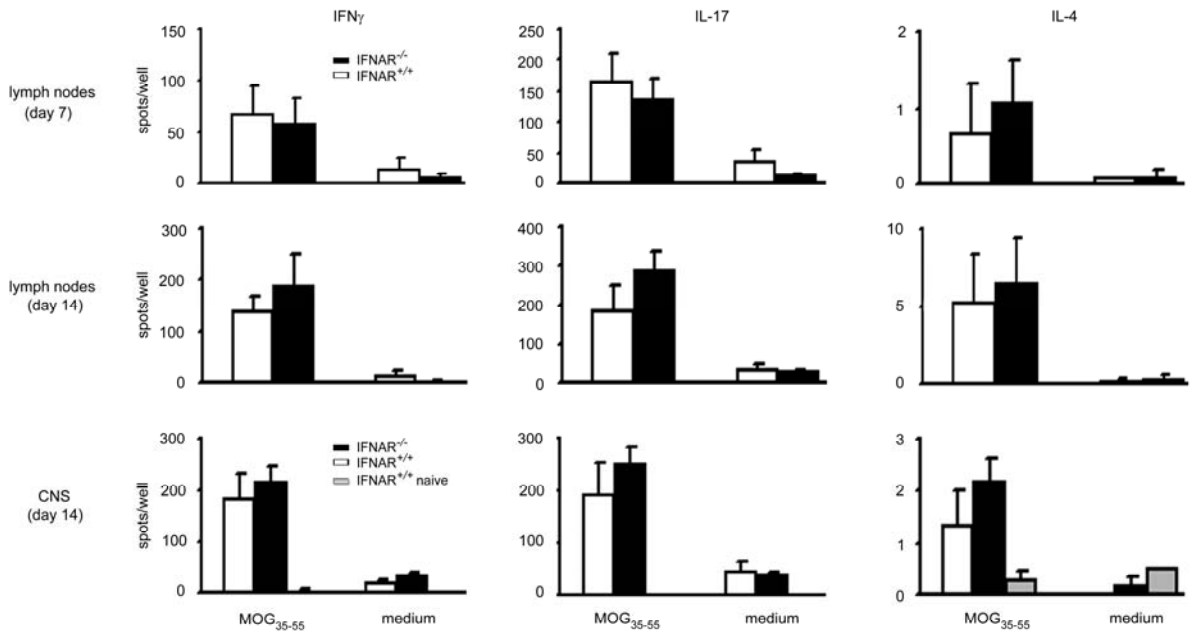

Figure S1. No Overt CD4 T Helper Subset Shift in the Absence of IFNAR
Quantification of the ELISPOT data shown in Fig. 2D. Lymph node and CNS-derived MOG-specific lymphocytes were harvested 7 or 14 days post immunization and IFN-γ, IL-4 and IL-17-producing spots were assessed quantitatively in a recall assay. Data show mean ± SEM. *Ifnar1*$^{-/-}$ (black bars) and *Ifnar1*$^{+/+}$ (white bars) animals are depicted.

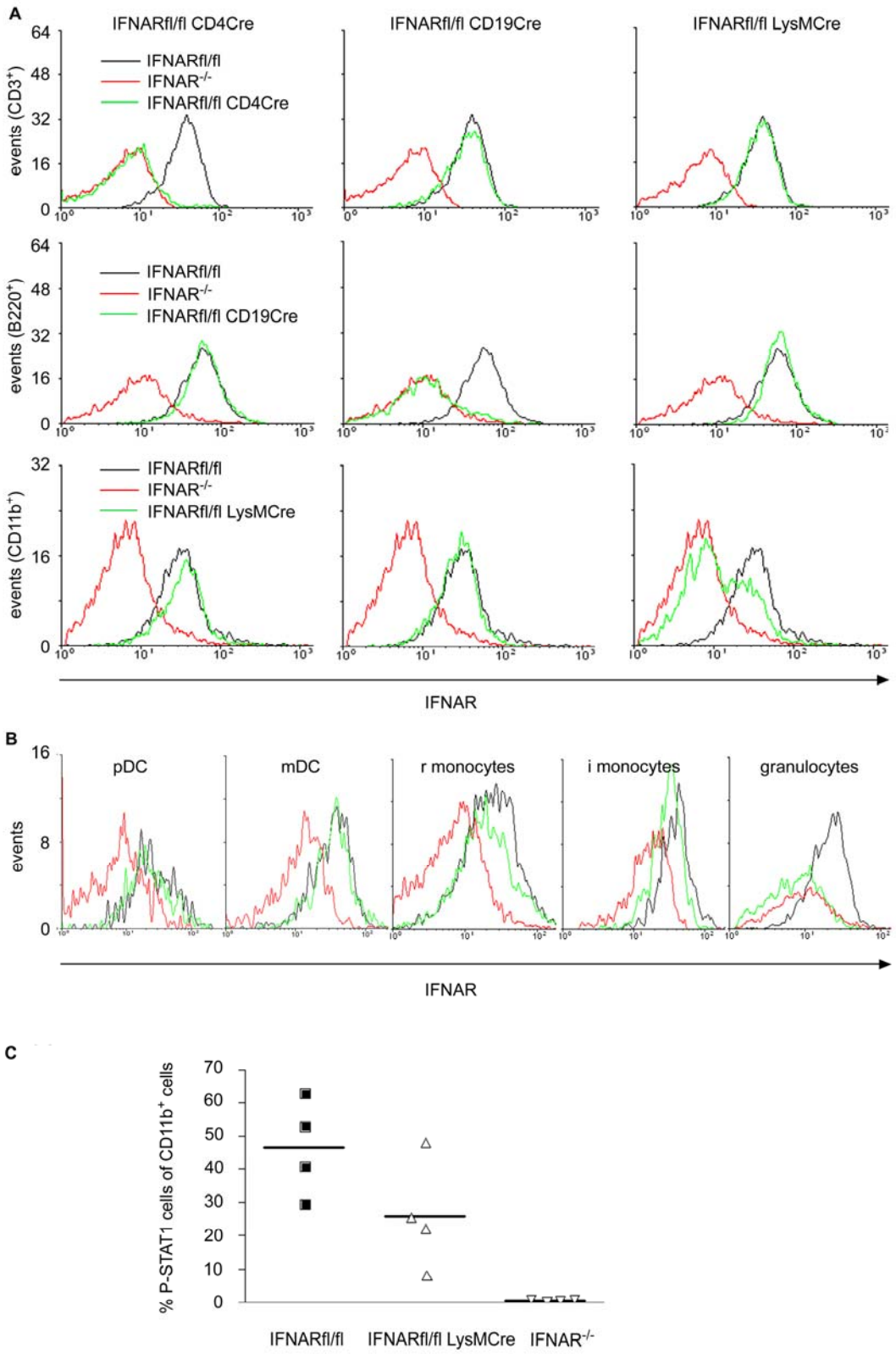

Figure S2. Cell-Type Specific Deletion of IFNAR in Several Cre Lines

(A) Flow cytometry using the anti mouse IFNAR antibody MAR1-5A3 indicates cell-type-specific and highly efficient IFNAR deletion in *Ifnar1*$^{fl/fl}$ CD4 Cre, *Ifnar1*$^{fl/fl}$ CD19 Cre and *Ifnar1*$^{fl/fl}$ LysMCre mice. Peripheral blood cells of 10 week old adult mice were stained with anti-CD3, anti-B220, anti-CD11b and anti-IFNAR, respectively. WT mice (*Ifnar1*$^{fl/fl}$, black lines) and *Ifnar1*$^{-/-}$ mice (red lines) were used as controls. Green lines indicate the respective Cre line used.

(B) Different degrees of IFNAR deletion on several CD11b$^+$ hematopoietic subsets such as CD11c$^+$CD11b$^-$B220$^+$ pDC, CD11c$^+$CD11b$^+$B220$^-$ mDC, Ly6C^{lo} resident monocytes (r monocytes), Ly-6C^{hi} inflammatory monocytes (i monocytes) and Gr-1$^+$ granulocytes. *Ifnar1*$^{fl/fl}$ LysMCre animals are visulalized with green lines, *Ifnar1*$^{-/-}$ with red lines and WT mice (*Ifnar1*$^{fl/fl}$) with black.
(C) Splenocytes were stimulated with 10 ng/ml IFN-β for 15 min and the percentage of phosphorylated STAT1 (P-STAT1) CD11b$^+$ cells was measured by FACS in *Ifnar1*$^{fl/fl}$ LysMCre, *Ifnar1*$^{-/-}$ and WT animals (*Ifnar1*$^{fl/fl}$).

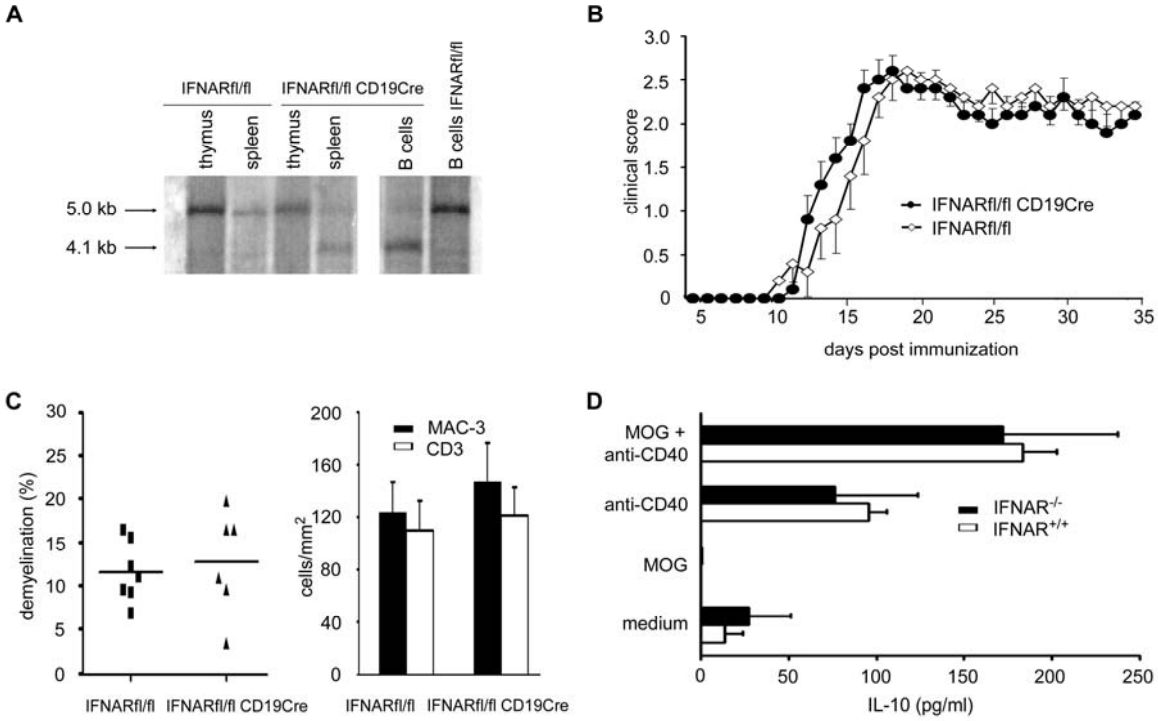

Figure S3. The Absence of IFNAR on B Cells Does Not Influence EAE Course and Concommitant CNS Pathology
(A) Southern blot reveals B-cell-specific IFNAR deletion in *Ifnar1*$^{fl/fl}$ CD19Cre mice.
(B) Active EAE in *Ifnar1*$^{fl/fl}$ CD19Cre mice (filled circles) and *Ifnar1*$^{fl/fl}$ (open squares) animals. One representative experiment out of two is shown.
(C) Normal histopathology of the CNS in *Ifnar1*$^{fl/fl}$ CD19Cre mice. The number of mononuclear cells infiltrating the spinal cord was assessed. MAC-3 for macrophages/microglia, CD3 for T lymphocytes and LFB for demyelination.
(D) B cells produce MOG-specific IL-10 in *Ifnar1*$^{-/-}$ (black bars) and *Ifnar1*$^{+/+}$ (white bars) mice. Medium alone was used as control. Data are given as means ± SEM from one representative experiment out of two.

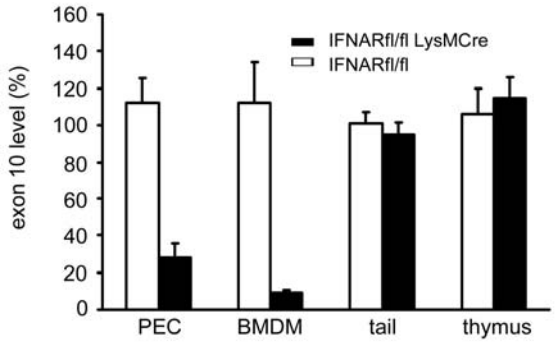

Figure S4. Specificity of Myeloid-Specific IFNAR Deletion in *Ifnar1*$^{fl/fl}$ LysMCre Mice
Quantification of exon 10 deletion in bone-marrow-derived macrophages (BMDM), thioglycollate-elicited peritoneal macrophages (PEC), tail and thymus of *Ifnar1*$^{fl/fl}$ LysMCre (black bars) and *Ifnar1*$^{fl/fl}$ (white bars) animals by real time-PCR.

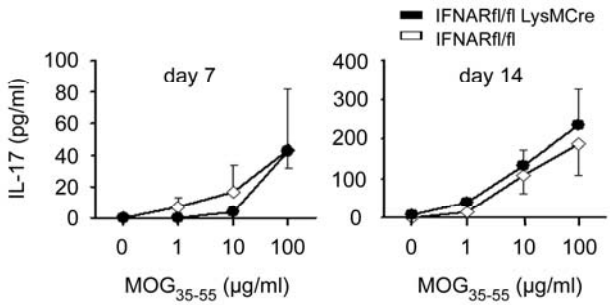

Figure S5. Normal Production of Encephalitigenic IL-17 in the Lymphoid Tissues of *Ifnar1*$^{fl/fl}$ LysMCre Mice
IL-17 production by MOG-specific lymphocytes after indicated time points was measured by ELISA. Data are given as means ± SEM and are supplemental to proliferation data depicted in Fig. 6C.

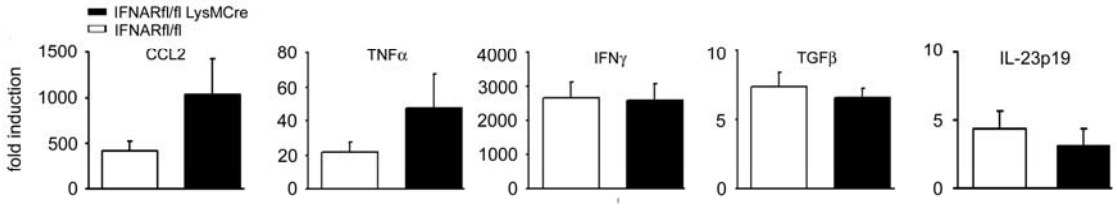

Figure S6. Cytokine and Chemokine Levels in the CNS of Myeloid-Specific *Ifnar1*$^{fl/fl}$ LysMCre Animals
Cytokine and chemokine profiles in the CNS of *Ifnar1*$^{fl/fl}$ LysMCre (black bars) and *Ifnar1*$^{fl/fl}$ (white bars) mice. mRNA was extracted at peak of disease and real-time PCR was performed. Data represent mean ± SEM. There are no statistically significant differences.

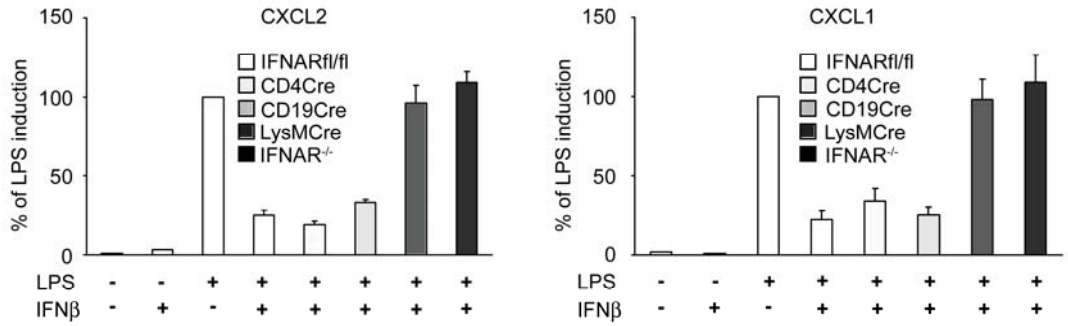

Figure S7. Changed Chemokine Production in the Absence of IFNAR on Macrophages
WT (*Ifnar1*$^{fl/fl}$), *Ifnar1*$^{fl/fl}$ CD4Cre, *Ifnar1*$^{fl/fl}$ CD19Cre, *Ifnar1*$^{fl/fl}$ LysMCre or *Ifnar1*$^{-/-}$ macrophages were exposed to either LPS alone or in combination with IFN-β and production of CXCL2 (MIP-2) and CXCL1 (GROα, KC) was measured by ELISA and compared to LPS-stimulated cells. Data represent mean ± SEM.

Table S1. The Presence of the Type 1 Interferon Receptor System Modulates Pathogenicity of EAE

Mouse genotypes	Incidence (%)	Lethality (%)	Mean day of disease onset (± SEM)	Mean maximal clinical score (± SEM)
Ifnar1$^{-/-}$	10/10 (100)	30*	13.4 ± 0.5	3.4 ± 0.1*
Ifnar1$^{+/+}$	10/10 (100)	0	14.1 ± 1.1	2.4 ± 0.3

One representative of four independent experiments is shown. *p<0.05

Table S2. Adoptive Transfer of MOG-Reactive Lymphocytes into *Ifnar1*$^{+/+}$ and *Ifnar1*$^{-/-}$ Recipients

Mouse genotypes	Incidence (%)	Mean day of disease onset (± SEM) [a]	Mean maximal clinical score (± SEM) [a]	Mean accumulative score (± SEM) [a]
Ifnar1$^{+/+}$	4/6 (67)	31.0 ± 2.8	2.2 ± 0.2	14.2 ± 5.5
Ifnar1$^{-/-}$	5/6 (83)	18.6 ± 2.7*	3.2 ± 0.3	53.0 ± 14.7*

The table summarizes data shown in Figure 3. [a] of diseased mice. *p<0.05

Table S3. Cell-Specific Requirement of the Type Interferon System during Autoimmune Encephalomyelitis

Mouse genotypes	Incidence (%)	Lethality (%)	Mean day of disease onset (± SEM) [a]	Mean maximal clinical score (± SEM) [a]
Ifnar1$^{fl/fl}$ NesCre	10/10 (100)	0	16.5 ± 1.5	2.6 ± 0.1
Ifnar1$^{fl/fl}$	8/9 (89)	0	13.6 ± 0.9	2.5 ± 0.4
Ifnar1$^{fl/fl}$ CD4Cre	6/6 (100)	0	13.3 ± 1.2	2.6 ± 0.2
Ifnar1$^{fl/fl}$	6/6 (100)	0	11.7 ± 0.5	2.3 ± 0.2
Ifnar1$^{fl/fl}$ CD19Cre	8/8 (100)	0	12.1 ± 0.9	2.9 ± 0.1
Ifnar1$^{fl/fl}$	8/8 (100)	0	14.9 ± 2.3	2.6 ± 0.3
Ifnar1$^{fl/fl}$ LysMCre	6/6 (100)	33*	14.8 ± 1.7	3.1 ± 0.1*
Ifnar1$^{fl/fl}$	6/6 (100)	0	12.7 ± 1.2	2.4 ± 0.2

The table shows a representative of at least two independent experiments for each experimental group. [a] of diseased mice. *p<0.05

Table S4.

Gene class	Gene symbol	fold change after 6 h	fold change after 24 h
IFN regulated genes *GO:0009615* *Response to virus* *p=5*10^{-10}*	IRF7	57.6	55.9
	Mx1	174.0	52.1
	STAT2	22.2	12.6
	STAT1	14.8	9.1
	Mx2	20.3	5.9
	IFIH1	15.0	7.0
	TLR3	13.7	4.1
	EIF2AK2	7.8	3.9
Antigen presentation *GO:0019882* *Antigen processing* *And presentation* *p=3*10^{-8}*	PSMB9	9.7	6.5
	PSMB8	5.1	4.2
	TAP2	7.7	3.1
	PSME1	2.8	2.7
	PSME2	3.2	2.2
	TAP1	16.1	9.0
	H2-D1	2.3	4.4
	TAPBP	4.8	3.9
Th1	IFNg	1.1	1.1
	IL12a	1.3	1.3
	IL12b	1.2	1.2
	IL12RB2	1.1	1.2
	STAT4	1.0	1.1
Th2	IL4	1.1	1.1
	STAT6	1.2	1.4
	IL13	1.2	1.1
Th17	IL23A	1.1	1.0
	IL17A	1.2	1.1
	IL17B	1.2	1.0
	IL6	2.4	1.0
	TGFB1	1.1	1.0
Chemotaxis *GO:0006935* *Chemotaxis* *p=0.00039*	CCL5	65.3	76.4
	CCL12	230.9	40.0
	CXCL10	154.8	10.6
	CCXL11	95.8	4.5
	CCL2	39.9	4.9
	CCL7	50.8	3.7
	CCL4	4.1	1.7
	CCL3	2.6	1.1
Other cytokines	IL-15	11.8	4.1
	IL-18BP	9.0	8.4
	TNFSF10	26.8	3.2
	IL-18	4.7	2.7
	TNFa	7.8	1.0

Selected genes in brain macrophages (microglia) after IFN-β (1.000 U/ml for 6h and 24h) treatment. IFN stimulated genes with a significant change in expression values between IFN-β treated and untreated samples (*p*-value <0.01) are shown in red. Corresponding Gene Ontology (GO) categories with the respective *p*-value are derived from a GO overrepresentation analysis for genes in cluster 1, 2 and 4 from Fig. 7D and shown in italics.